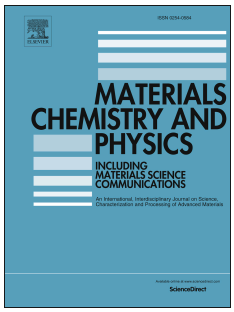

Photocatalytic performance of a novel semiconductor nanocatalyst: Copper doped nickel oxide for phenol degradation

Anita Sagadevan Ethiraj, Prateek Uttam, Varunkumar K, Kwok Feng Chong, Gomaa A.M. Ali

PII: S0254-0584(19)31330-6

DOI: https://doi.org/10.1016/j.matchemphys.2019.122520

Reference: MAC 122520

To appear in: *Materials Chemistry and Physics*

Received Date: 20 May 2019

Revised Date: 30 November 2019

Accepted Date: 2 December 2019

Please cite this article as: A.S. Ethiraj, P. Uttam, V. K, K.F. Chong, G.A.M. Ali, Photocatalytic performance of a novel semiconductor nanocatalyst: Copper doped nickel oxide for phenol degradation, *Materials Chemistry and Physics* (2020), doi: https://doi.org/10.1016/j.matchemphys.2019.122520.

Photocatalytic performance of a novel semiconductor nanocatalyst: Copper doped nickel oxide for phenol degradation

Anita Sagadevan Ethiraj [1, 2,]*, Prateek Uttam [2], Varunkumar K. [2], Kwok Feng Chong [3], Gomaa A. M. Ali [3,4,]

Graphical Abstract:

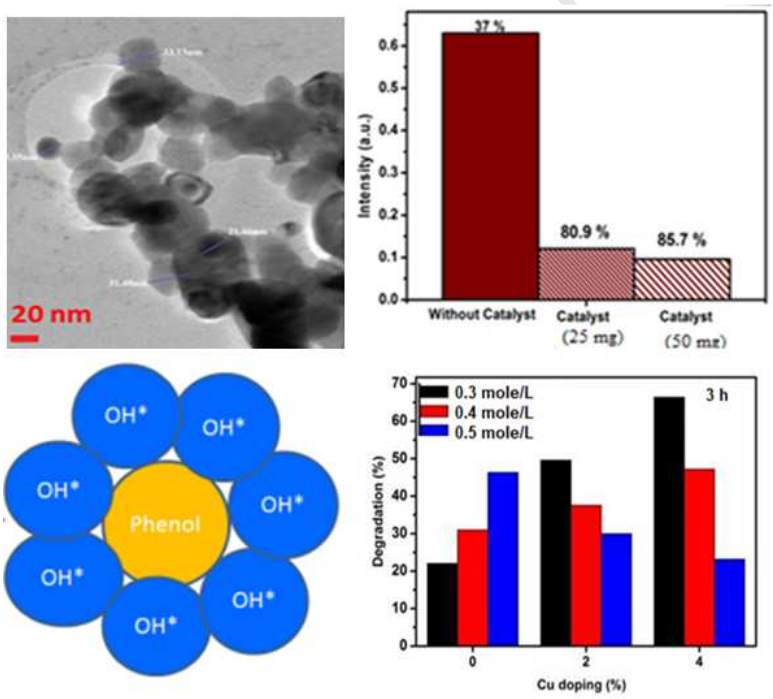

Photocatalytic performance of a novel semiconductor nanocatalyst: Copper doped nickel oxide for phenol degradation

Anita Sagadevan Ethiraj [1, 2,]*, Prateek Uttam [2], Varunkumar K. [2], Kwok Feng Chong [3], Gomaa A. M. Ali [3, 4]

[1]*Department of Physics, VIT-AP University, Amaravati, Andhra Pradesh 522237, India*

[2]*Centre for Nanotechnology Research, VIT University, Vellore - 632 014, Tamil Nadu, India.*

[3] *Faculty of Industrial Science & Technology, Universiti Malaysia Pahang, Gambang, 26300 Kuantan, Malaysia*

[4]*Chemistry Department, Faculty of Science, Al-Azhar University, Assiut 71524, Egypt*

***Corresponding Author:** Dr. Anita Sagadevan Ethiraj, Associate Professor,

Department of Physics, VIT-AP University, Amaravati, Andhra Pradesh 522237, India

E-mail: ethirajanita25@gmail.com

(M): 7397609870

Abstract

In this study, the degradation of phenolic compounds was performed in the presence of pure and Cu doped nickel oxide (Cu-NiO) nanocatalysts. A wet chemical method was utilized for the catalyst preparation. The crystallinity and phase were determined using X-ray diffraction, optical properties were analyzed by UV-Vis spectroscopy and morphology was analyzed by a transmission electron microscope. Fourier transform infrared spectroscopy confirms the formation of pure NiO and the existence of copper in doped nanocatalyst samples. Cu-NiO nanocatalyst samples showed a reduction in average crystallite size as compared to pure NiO sample, where it was 24.0, 22.8 and 19.03 nm for 2Cu-NiO and 4Cu-NiO, respectively. The average particle size as determined by using transmittance electron microscopy were about 28.0, 26.6 and 22.8 nm for NiO, 2Cu-NiO and 4Cu-NiO, respectively. In addition, the energy bandgap values were found to be 3.26, 3.64 and 3.87 eV for undoped NiO, 2Cu-NiO and 4Cu-NiO, respectively. Comparative study of the photocatalytic performance of Cu-NiO and pure NiO were systematically performed at various reaction times and Cu doping ratios (2-4 wt. %). Different molar concentrations of phenol were also considered for this study. The obtained results showed that the Cu-NiO nanocatalyst exhibited the highest phenol degradation efficiency as compared to their undoped counterpart. This material is first reported and successfully used in efficient removal of phenol from real industrial effluent. The nanocatalyst efficiency for phenol removal was tested in real leather industrial wastewater effluent which could remove about 85.7% within 150 min.

Keywords: Copper doped NiO, Nanocatalyst, Photodegradation, Phenol, Water treatment

1. Introduction

Water pollution is a serious problem to the whole world; therefore, much effort has been given for water purification and pollutants removal [1-3]. In the last few decades contaminations due to phenolic compounds in the industrial wastewater were reported to be high [4]. Phenolic compounds were identified as hazardous pollutants to the environment and human beings. Even its contamination existing in few ppm levels reflects severe carcinogenic to humans and other living species [5-7]. Therefore, removing of phenolic compounds from industrial wastewater is necessary and interesting. Many studies reported on photodecomposition of phenol compounds using semiconductor nanoparticles (NPs) as a catalyst [8-11]. In addition, different methods such as microwave enhanced advance oxidation process catalytic oxidation [12-15], catalytic oxidation [16], ultrasonic degradation [17], sonochemical degradation [18], photocatalytic degradation [19-22], photo-Fenton degradation photo-Fenton [23], photoelectrocatalytic degradation [24], photodecolorization [25] and adsorption [26] have been utilized.

Ba-Abbad *et al.* prepared TiO_2 NPs via the sol-gel method and tested for degradation of chlorophenols (2-chlorophenol (2-CP), 2,4,6-trichlorophenol (2,4,6-TCP) and 2,4-dichlorophenol (2,4-DCP)). The degradation ratio was about 99, 98 and 92% for 2-CP, 2,4-DCP, and 2,4,6-TCP, respectively, at 50 mg/L, 90 min. of irradiation [27]. When the initial concentration was greater than 50 mg/L, the degradation ratio and rate constant (K_{app}) was decreased [27]. In addition, Wang *et al.* synthesized carbon-incorporated mesoporous NiO/TiO_2 hybrid shells, using polystyrene nanospheres as templates and tested photoactivity by the degradation of organic pollutant (Rhodamine B, Methylene Blue, and Phenol). Initially, the calcination temperature of catalysts was controlled at 500, 600, 700, 800 and 900 ^oC. Among these, the catalyst calcinated at 800 ^oC reported as the highest photocatalytic activity under irradiation of visible light. The

initial concentration of organic pollutes (Methylene Blue or Rhodamine B) and phenol was $2x10^{-5}$ and 10 mg/L, respectively. Degradation ratio was about 98, 94 and 88% for Methylene blue, Rhodamine B and phenol at 75, 100 and 150 min., respectively. Stability of materials had confirmed by running 6 successive cycles and it showed excellent photoactivity end of the 6th cycle [28]. A comparison study of advanced oxidation processes (photolysis and UV/H_2O_2, ozone and its combination, Fenton and photocatalysis) was reported, it also includes optimum oxidant/pollutant ratio, pH influence, stoichiometric coefficient and kinetic constant. Among all these tested processes, it was found that the lower cost processes are ozonation, none of the ozone combinations (O_3/H_2O_2, O_3/UV/H_2O_2, and O_3/UV) degradation rate. While, in case of UV processes (photocatalysis, UV and UV/H_2O_2), the degradation rate of UV/H_2O_2 was almost 5-times higher than UV and photocatalysis alone, Fenton reagent was the faster degradation. In comparison, Fenton degradation was 40-times higher than UV and photocatalysis and 5-times higher than ozonation [29].

Carbon/nitrogen-doped TiO_2 porous nanocrystalline photocatalyst with the particle size of 35-40 nm was reported for phenol degradation. Degradation ratio was about 64 and 57% for photocatalysts C/N-doped TiO_2 and TiO_2, respectively, at 60 min. of UV irradiation. The total amount of phenol degraded was about 87% at irradiation of 90 and 150 min, this was due to the accumulation of CO_2 on surfaces of C/N-doped TiO_2 [30]. Sharma and Lee have reported on TiO_2/NiO/RGO nanocomposite as a photocatalyst, which was synthesized by in-situ sol-gel process. They have achieved 88.4% of photodegradation using 100 mg/L 0-chlorophenol at pH-6.5, 8 h of visible light irradiation and with the addition of 0.01% H_2O_2. The photocatalyst was stable after 4 successive cycles and it retained a high degradation ratio [31]. $NiFe_2O_4$/multi-walled carbon nanotubes ($NiFe_2O_4$/MWNT) were prepared by the single step hydrothermal

process. It's also showing the magnetically recyclable and high photocatalytic property [32]. Labiadh *et al.* synthesized Cu doped ZnS quantum dots via a hydrothermal method with an average diameter of 2.9 nm. TiO_2/Cu:ZnS was the highest photocatalytic activity than TiO_2/ZnS nanocomposites, which showed higher photoactivity performance towards the pollutant salicylic acid [33]. NiO supported on clinoptilolite nanoparticles (20-44 nm) showed high photocatalytic activity of cotrimaxazole pharmaceutical capsule [34]. Moreover, Hayat *et al.* have reported on cubic NiO nanoparticles with average crystallite size is about 6-10 nm, synthesized by sol-gel method. It has been utilized for phenol degradation and they attain high degradation efficiency of about 97% under UV laser irradiation and initial concentration of phenol solution was 100 mg/L [35].

To best of our knowledge, this is the first time Cu doped NiO as nanocatalyst is used for photodegradation of phenol. The synthesized Cu doped NiO nanocatalyst has been utilized for phenol degradation. Detailed structural and morphological studies were performed to deeply understand the photodegradation process and mechanism.

2. Materials and methods

2.1. Materials

Phenol (99%) was procured from Sigma-Aldrich. The chemicals were stored at 21 °C, and stock preparations were prepared when it is needed. Nickel chloride hexahydrate ($NiCl_2.6H_2O$), copper sulfate pentahydrate ($CuSO_4.5H_2O$) and sodium hydroxide (NaOH) were also procured from Sigma Aldrich and were used without further purification. Ultrapure deionized water was used as the reaction medium in all the synthesis steps.

2.2. Nanocatalysts synthesis

Nickel oxide NPs was synthesized by a wet chemical method. $NiCl_2.6H_2O$ (2.37 g in 100 mL distilled water) was stirred for 30 min. Then NaOH (2 g in 100 ml) was used to adjust the pH 10. Later green precipitate was obtained, washed with distilled water and ethanol to remove any impurities. The precipitate was dried in an oven at 60 ^oC for 14 h for the removal of hydroxyl radicals and subjected to an appropriate temperature to obtain the final product [36]. A similar method was adopted to prepare the doped NPs except for the addition of $CuSO_4.5H_2O$ (2 wt. % (0.063 g) and 4 wt. % (0.127 g) along with $NiCl_2$. $6H_2O$ during the synthesis process. Obtained 0, 2, and 4Cu-NiO samples were labeled as NiO, 2Cu-NiO, and 4Cu-NiO.

2.3. Catalytic degradation of phenol

Photocatalytic reactions were performed using Heber multi-lamp photo reactor chamber installed with 150 W high-pressure UV lamp operated at 254 nm wavelength. The degradation experiment was done using 100 mL of aqueous phenol solutions with an initial concentration of 0.3 (2.82 g), 0.4 mol/L (3.76 g) and 0.5 mol/L (4.7 g) and 0.25 g of prepared nanocatalyst (NiO, Cu doped NiO). For each experimental run, the phenol solution was saturated by bubbling O_2 for 10 min. before the addition of catalysts (before the addition of catalysts). In each run, after the mixture of 0.25 g of catalysts in 100 mL of aqueous phenol solutions was reposed at dark for 30 min., the light was turned on to initiate the degradation process. A UV- Visible spectrometer was used to determine the concentration of phenol solution after the photocatalytic degradation experiment was conducted for different time intervals (3 and 5 h).

3. Results and discussion

3.1. X-Ray diffraction analysis

The XRD patterns of NiO, 2Cu-NiO, and 4Cu-NiO are shown in Fig. 1. The peaks at 2θ of 37.57, 43.60, 63.10, 75.57 and 79.62° are related to pure NiO and corresponded to (111), (200), (220), (311) and (222) planes [37]. In the case of Cu doped NiO, the position of the peak was slightly shifted to lower angles (37.01, 43.05, 62.69, 75.28 and 79.27°) [36]. All these diffraction peaks were in accordance to that of the standard spectrum (card No. 01-073-1523, 01-078-0646 and 01-078- 0648) of NiO [36]. From the XRD analysis, it is identified that the prepared samples were in a cubic phase. The average crystallite size of the NiO nanoparticles was estimated from the full width half maximum (FWHM) and the peak position according to the Scherrer formula [38]. Average crystallite size for pure, 2Cu-NiO and 4Cu-NiO was about 24.0, 22.8 and 19.03 nm, respectively [39]. Since the Cu doping is in low amount, it could not be detected by XRD.

3.2. Transmittance electron microscopy and energy-dispersive X-ray spectroscopy analyses

Transmittance electron microscopy (TEM) image for NiO is shown in Fig. S1a, where it shows spherical agglomerated nanoparticles [40]. The energy-dispersive X-ray spectroscopy (EDS) spectrum (Fig. S1b) identifies the presence of Ni and O. The presence of C as an impurity is from the system. Figs. 2a and 2b depict the TEM micrographs for 2Cu-NiO and 4Cu-NiO. For 2Cu-NiO, it shows that the nanoparticles have spherical like form with a diameter in the range of 20-35 nm including large agglomerates. In the case of 4Cu-NiO, dense, agglomerated particles in the range of 19-33 nm were seen with few well-faceted particles as shown in the inset of Fig. 2b. In the present case, the observation of some large nanoparticles may be attributed to the fact that the high surface energy and tension making Cu doped NiO NPs have a tendency to

agglomeration [41, 42]. The selective area electron diffraction (SAED) patterns of 2Cu-NiO and 4Cu-NiO are shown in Figs. 2c and 2d, indicate the polycrystalline nature of prepared nanomaterials. The strong electron diffraction rings can be assigned to (111), (200), (220), (311) and (222) planes, as a result, the HR-TEM and SAED analyses confirm the crystalline nature of synthesized pure and Cu doped NiO NPs with cubic structure. Figure 2e and 2f confirms the presence of Cu in the doped samples. Moreover with an increase in the percentage of Cu doping the intensity of Cu peak in EDS increased. The average particle size as determined by using TEM data were found to be about 28.0, 26.6 and 22.8 nm for NiO, 2Cu-NiO and 4Cu-NiO, respectively. The results clearly show that the mean particle size estimated by TEM is in good agreement with the average crystallite size determined from the XRD data.

3.3. Ultraviolet–visible spectroscopy analysis

Ultraviolet–visible (UV-Vis) absorption spectra of as-synthesized NiO, 2Cu-NiO, and 4Cu-NiO are shown in Fig. S2a. The absorption peaks were observed at 380, 340 and 320 nm respectively for these samples. The results clearly indicate a blue shift in the absorption spectra with the increase in Cu content which could be attributed to the quantum size effect. The band gap was calculated from the absorption edge wavelength by using the following equation [41-43]. As we know, the more precise method for the calculation of band gap energy is using of Kubelka-Munk equation and the resulted Tauc plots that are discussed in more details in literature [44-47].

$$E_g = \frac{1240}{\lambda} \quad (1)$$

Bandgap results, average crystallite size calculated by Debye-Scherrer and the particles size determined by TEM analysis are listed in Table 1.

3.4. Fourier Transform Infrared spectroscopy

Fig. S2b highlights the FTIR spectra of NiO, 2Cu-NiO, and 4Cu-NiO in the range of 4000-400 cm^{-1}. The broad absorption band observed at 3500 cm^{-1} corresponds to O-H bond stretching vibration of the interlayer water molecules and hydroxyl groups [48-50]. The nanocrystalline nature of the synthesized nanoparticles is evident from the broadness of the absorption band. The CO_2 vibration bond due to the presence of air was observed at 2380 cm^{-1}[51] . The band at 1643 cm^{-1} due to O-H bending vibrations is also observed in doped NiO NPs [52]. In the wavenumber region of 1050-1200 cm^{-1}, the observed peaks may be attributed to the presence of carbonates. The intensity of these peaks was found to increase with the increase in Cu doping. The prominent peak was observed at 531 cm^{-1}, which indicates the Ni-O stretching mode [39, 53, 54]. While 644 cm^{-1} denotes the vibration due to the Cu-O stretching band [55, 56].

3.5. Phenol degradation

The phenol degradation using pure NiO and Cu doped NiO nanocatalysts under pH 10 and different phenol concentrations (0.3, 0.4 and 0.5 mol/L), UV light exposure time (3 and 5 h), a constant amount of oxygen dissolved and respective UV–Vis spectra are discussed. The phenol degradation experiments were conducted in UV photoreactor chamber with initial passing of O_2 into the phenol solution to enhance the phenol degradation [57, 58]. Based on Petrov *et al.* findings, phenol degradation was slow in absence of O_2, here we conducted the experiment in presence of O_2 and phenol UV absorption peak wavelength has observed in 210 to 230 nm. The respective phenol solutions, two peaks wavelengths were about 200 and 210 nm [41].

The UV absorption spectra of different phenol concentrations in the absence of catalysts with two different reaction times are shown in Fig. S3. It was found that phenol has been left intact

under oxygen (O_2) in the absence of catalyst by observing two intense and broad maximum absorption peaks at 210 and 270 nm. Petrov *et al.* reported the initial peak positions wavelength of phenol solutions were 200 and 270 nm respectively and in the absence of the catalyst, oxidation of phenol was very slow [41].

The effect of catalysts at two different durations and different phenol concentrations were studied by adding 0.25 g of catalysts in 50 mL of phenol aqueous solutions. From the UV-Vis spectra shown in Fig. S3, it clearly is seen that phenol degradation proceeded substantially after exposure to oxygen in the presence of a catalyst (0% Cu-doped NiO), reduction in phenol concentration through oxidation reaction, supported degradation curve was observed a reduction in the intensity of phenol broad peak at 210 and 270 nm. The phenol degradation (%) was calculated from equation (2) [8, 59]:

$$Phenol\ degradedation\ (\%) = \frac{C_o - C_t}{C_o} * 100 \qquad (2)$$

Where C_o and C_t denote the phenol initial concentration and at time t.

At the end of 3 h reaction time, the degradation efficiency was about 22.05, 30.56 and 46.31% achieved for 0.3, 0.4 and 0.5 mol/L, respectively. While the phenol degradation efficiency was about 44.96, 40.80 and 64.05% for 5 h reaction time for 0.3, 0.4 and 0.5 mol/L, respectively. Using NiO as nanocatalysts, the highest degradation efficiency was 46.00 and 64.05% in the cases of 3 and 5 h, respectively, for 0.5 mole/L.

UV-Vis curves with respect to phenol concentration 0.3, 0.4 and 0.5 mol/L and the addition of nanocatalysts doped 2Cu-NiO and 4 Cu-NiO are shown in Fig. 3 (for pure NiO it is shown in Fig. S4). The 2Cu-NiO has accelerated the oxidation rate of phenol, compared to pristine NiO.

This might be due to the physical structure of the catalyst, NiO has its absorption wavelength in the UV region. The observed phenol degradation efficiency was 49.61, 37.55 and 30.00% for 3 h for 0.3, 0.4 and 0.5 mol/L, respectively. In the duration of 5 h, the phenol degradation efficiency was 58.77, 75.2, and 72.04%, respectively for 0.3, 0.4 and 0.5 mol/L. It has been reported that the low photoactivity arises, which was because of structural imperfections in the pristine NPs generate trap sites, results decrease the level of electrons and holes. In metal-doped NPs, doped ions result as charge trapping sites and reduce the recombination rate which leads to enhance the photoreactivity [4]. Rengaraj and Li reported on mineralization of 2, 4, 6 trichlorophenol under UV illumination, with Ag-doped TiO_2 as a catalyst. They found the degradation was more than 95% in 120 min. [60].

On the other hand, 4Cu-NiO has not accelerated the oxidation rate of phenol as much as compared to NiO and 2Cu-NiO. The photodegradation efficiency was 66.38, 47.20 and 23.15% (3 h) and 66.83, 46.56 and 56.70% (5 h) for 0.3, 0.4 and 0.5 mol/L, respectively. It's clearly observed, doped catalyst showing higher phenol degraded efficiency comparatively than NiO, at 5 h reaction time. The nanocatalyst photocatalytic activity increases with respect to the bandgap. The higher degradation of phenol was using 2Cu-NiO doped samples which has a bandgap of 3.64 eV [61]. These were renowned, optical properties of Cu doped NiO have effects on photoreactivity with respect to the light absorption efficiency [62]. Here all the cases photoreactivity of Cu doped NiO samples correspondence phenol degradation efficiency has comparably improved than pristine NiO. This may be arises due to increased photogeneration, the rate of charge transfer between Cu^{2+} electrons and NiO conduction or valence band [63]. Burns *et al.* carried out an investigation on Nd-doped TiO_2 used for photodegradation of 2-chlorophenol under UV irradiation. Their result shows that degradation time has been reduced,

due to the difference between ionic radii of TiO_2 and Nd^{3+}. Active sites and photoabsorption of the catalyst were two imperative needs, which involved in the photodegradation of pollutants [64]. The 2Cu-NiO catalyst showed improved performance than undoped degradation rate. When the Cu doping content was reached 4 wt.%, the photocatalytic activity was not improved as such compared to 2Cu-NiO [65].

3.6. Photocatalytic activity of phenol

The efficiency of phenol degradation as a function of varies the experimental parameters was shown in Figs. 4 and 5. In the comparison study of photocatalytic activity, *via* wet chemical prepared materials consents to settle on that excepting the use of copper in all the cases. Photocatalytic efficiency has been observed for phenol degradation using undoped NiO, 2Cu-NiO, and 4Cu-NiO as nanocatalyst at the 3 h of reaction time was shown in Fig. 4. In that different doping wt. % of Cu, it is observed undoped pristine NiO material shown 46.31% in 0.5 mol/L. Thus 2Cu-NiO and 4Cu-NiO were shown higher degradation efficiency of about 49.61 and 66.38 % at 0.3 mol/L of phenol concentrations, respectively. The concentrations of phenol were lower, and it may also affect the phenol degradation. Obviously, it shows higher phenol concentration with respect to the lower concentration of phenol. These results are matched with the published reports [66]. It has recommended that the initial concentration of phenol directly influence both degradation and conversion rate of phenol in the range of 0.1-1 g/L. When it exceeds 1 g/L, catalysts relative activity has decreased. It takes a long time to degrade when the phenol concentration was much higher [67].

The photodegradation efficiency versus time plot of phenol has been done for different phenol concentrations during 5 h reaction time as shown in Fig. 5. The observed maximum phenol degradation efficiencies were about 64.05% for the NiO at 0.5 mol/L. In the case of doped samples, 75.2 and 66.83% were observed to be high phenol degradation efficiency for 2Cu-NiO at 0.4 m/L and 4Cu-NiO at 0.3 m/L. The highest degradation efficiency was noticed in 0.4 mol/L and 0.3 mol/L, which was lower than 0.5 mol/L concentration of phenol [66]. The photocatalytic activity was improved for doped material when comparing to the undoped material after 3 h and 5 h reaction of duration time [61].

High dosage affects the degradation rate because it's reduced light penetration [68]. The degradation efficiency of phenol has higher for low concentrations, which was observed in 2Cu-NiO, while 4Cu-NiO has shown higher degradation efficiency in 0.3 mol/L [66]. It's been concluded oxidation of phenol in the absence of catalyst takes a very long time [41].

In order to study the comparison of different catalyst activity and chemical process, it was necessary to know the kinetics study. Earlier, researchers including Gondal *et al.* and Judi *et al.* have described the kinetics of photocatalytic degradation of phenol by Langmuir-Hinshelwood equation. It directly relates to the degradation rate (r) and the concentration of phenol (C), which was expressed as follows [59, 69-71].

$$r = -\frac{dc}{dt} = \frac{kKC}{1 + KC} \tag{3}$$

Here, C is the phenol concentration at irradiation time 't', k represents the reaction rate constant which normally depends on various experimental parameters such as the quantity of photocatalyst, photonic efficiency, incident laser energy, and K is adsorption constant of phenol

on the surface of the catalyst. When the initial phenol concentrations were low enough, equation (3) simplified as following pseudo-first-order kinetics and equation was followed as:

$$-ln\frac{C_t}{C_0} = K_{app}t \quad (4)$$

Where apparent first-order rate constant K_{app} ($min.^{-1}$) corresponds to the photocatalysis photodegradation rate. K_{app} can be determined by plotting $-ln\frac{C_t}{C_0}$ vs. *t*. It will give the straight line, and the slope is apparent rate constant K_{app}. Ye and his co-workers applied the equation 4, when they studied phenol concentrations were 10 mg/L to 60 mg/L [69]. Hayat et al. have varied initial phenol concentration from 50 mg/L to 250 mg/L and they used equation (4) [35]. Here in this work, initial phenol concentrations were varied from 1.41 g/L to 2.35 g/L. Equation 4 was applicable for low concentrations and therefore we concerned the method to the following pseudo- first order kinetics.

The effects of phenol initial concentrations on the K_{app} values acquired in the degradation with respect to different concentrations of phenol within 180 min. and 300 min. were shown in Figs. 6 and 7 respectively. In the reports of Labbe *et al.* mentioned the least squares regression values (r^2) for the degradation rate constant of phenol photocatalysis ($r^2 > 0.9372$) recommend a reasonably good fit between $-ln\frac{C_t}{C_0}$ vs. *t* [72].

First order rate constant and the regression coefficient have been determined from the plot. First order rate constant and regression coefficients, which were directly related to varying the initial phenol conc. and Cu doped NiO has been shown in Table 2. The obtained r^2 values were higher than 0.9372 [72].

Fig. 7 shows the plot $-\ln (C_t/C_o)$ vs. t with respect to the 5 h of reaction irradiation time. From the $-\ln (C_t/C_o)$ versus time plot, one can calculate the K_{app} rate constant. First order rate constant

and respective regression coefficient for 3 and 5 h reaction time were shown in Table 2. In Fig. 7 and Table 2 clearly demonstrates in all the cases Cu doped has higher K_{app} values than pristine NiO. From Table 2, it was clearly displayed at higher initial phenol concentration K_{app} values of doped samples was also observed to be lower.

Fig. 8 shows the comparative histogram of Cu doping versus degradation efficiency of phenol with respect to 0.3, 0.4 and 0.5 m/L of phenol concentration for 3 and 5 h of irradiation reaction times, respectively. In the case of 3 h of irradiation reaction time, maximum phenol degradation efficiency was 66.38 and 47.20% observed for 4Cu-NiO, both the cases of 0.3 and 0.4 mol/L. In the case of 0.5 mol/L phenol concentration, maximum degradation efficiency 46.31% was seen in undoped NiO samples. While for 5 h reaction time maximum phenol degradation efficiency was about 66.83, 75.2 and 72.04% as seen in NiO, 4Cu-NiO and 4Cu-NiO samples on phenol concentrations of 0.3, 0.4 and 0.5 mol/L, respectively.

Therefore, when a high amount of Cu^{2+} ions were doped, they can entrap the photo induced electrons to form Cu^{+} ions. Since $\varphi 0(Cu^{2+}/Cu^{+})=0.16$ V (vs NHE), while $\varphi 0(Cu^{2+}/Cu^{+})=0.25$ V (vs NHE). Formed Cu^{+} ions can detain the photoinduced holes and generate Cu^{2+} [73]. As a result, short-circuiting forms and both photoinduced electrons and holes were consumed. Consequently, these were reduced the photocatalytic activity. Therefore, Yang *et al.* have also reported optimum Cu content (1.0%) at which the Cu-doped TiO_2. To separate effectively the photoinduced electron-hole pair 1% Cu content was adequate, compared to higher Cu contents and achieved the best photocatalytic performance [65]. Here in this study, we have also observed the best photocatalytic activity at 2Cu-NiO compared to 4Cu-NiO.

The K_{app} apparent rate constant of different concentrations of phenols for NiO were 0.00136, 0.00203 and 0.00346 min^{-1}, for 2Cu-NiO were 0.00382, 0.00266, and 0.00200 min^{-1}, for 4Cu-

NiO were 0.00603, 0.00353 and 0.00144 min^{-1} for 0.3, 0.4 and 0.5 mol/L, respectively, in 3 h irradiation time. In case of 5 h irradiation time, K_{app} values were 0.00198, 0.00175 and 0.00342 min^{-1} for for NiO, 0.00296, 0.0047 and 0.00425 min^{-1} for 2Cu-NiO and 0.00365, 0.00209 and 0.00276 $min.^{-1}$ for 2Cu-NiO, respectively, 0.3, 0.4 and 0.5 mol/L.

Table 3 shows a comparison of NiO, 2Cu-NiO, and 4Cu-NiO with its respective phenol degradation efficiencies. It is clearly shown Cu doping and phenol concentration has a significant role in an increasing the phenol degradation efficiency. High initial phenol concentrations required long degradation time.

3.7. Mechanism of degradation

The bulk quantity of species including $O_2^{\bullet}$, h_{vb}^{+}, $^{\bullet}OH$ was engrossed for the photocatalytic process. Cu doping helps to prevent the recombination of photogenerated electron-hole pairs which leads to decrease the photodegradation efficiency [74-76]. Two different reaction times and different ratios of doped samples were explored in an endeavor to reveal the mechanism photocatalytic process [77, 78].

As prepared Cu doped nanocatalysts show a positive effect on the photocatalytic activity of phenol degradation. The possible mechanistic photodegradation of phenol by Cu doped NiO nanocatalysts was shown in Fig. 9. Photocatalytic activity reaction occurs only at highly activation UV irradiation incident on catalysts. The electrons were ascended up from lower energy (valence band) to higher energy (conduction band) while leaving in the rear charge separation as results of positively charged holes. But these electrons and holes recombine quickly, it leads to suppressing the photoactivity of the catalyst. It will be overcome by means of transition metal doping. Thus, Cu doping extends light harvesting both UV and visible regions,

first. In second Cu species acts as electron scavenger, results at the contact region of the semiconductor-metal Schottky barrier formed, which assists the charge separation and enhance the photoactivity performances. The efficient separation of photoinduced electron-hole pairs was possible due to induced energy levels by impurity doping. Since Cu^{2+} ion was less than that of Ni^{2+}, doping of Cu induces oxygen vacancies, which acts as active sites for water dissociation on the surface of NiO and also capture the holes to restrain recombination of electron-hole pairs. The Cu^{2+} ion was superior to O_2 in its competent of trapping electrons ($Cu^{2+} + e^- \leftrightarrow Cu^+$). The electrons trapped in Cu^{2+} sites can transfer to the adsorbed O_2 via an oxidation process ($Cu^+ + O_2 \leftrightarrow Cu^{2+} + O_2^-$) and produces superoxide radical anion (O_2^-). Meanwhile, the holes in the valence band of NiO react with immanent H_2O molecules to produce highly reactive hydroxyl radicals ($^\bullet$OH) [74]. The highly reactive hydroxyl radicals and superoxide radical anion lead to degradation of phenol. The increase in separation of electron-hole pairs, results increase in production of O_2^- and $^\bullet$OH by Cu increases the photoactivity of Cu doped NiO [65, 79, 80].

3.8. Leather industries phenol real effluents

In order to determine the photocatalytic activity of as prepared nanocatalyst, the samples were tested with leather industries real effluents, which have major phenol content obtained from leather industry in karai, puliankanu (Sipcot) at Ranipet. Fig. 10 illustrates the absorption spectrum of the real effluent with the inset depicting the picture of the leather industries real effluent sample. These nanocatalysts showed positive results and high photocatalytic activity on real effluents, which has been taken from leather industries. The observed phenol degradation UV-Vis spectra were shown in Fig. 11. From the spectra degradation efficiency has calculated, these were about 81.53 and 86.15% for 25 mg and 50 mg of catalyst, respectively, utilized for

degradation of real phenol effluents, which observed at 150 min. The comparison of UV-Vis degradation spectra of leather industry wastewater (real effluents) and phenol are shown in Fig. S5. The maximum degradation of real effluents intensities was shown in the form of the histogram as inset.

4. Conclusions

Cu doped NiO nanocatalysts have been successfully prepared and applied for phenol photodegradation. The nanocatalysts were characterized by XRD, UV-Vis spectroscopy, IR spectroscopy, and transmission electron microscope. The average crystallite sizes were 24, 22 and 19 nm for undoped NiO, 2Cu-NiO, and 4Cu-NiO, respectively, and match with the particle size of TEM. Energy bandgaps were found to be 3.26, 3.64 and 3.87 eV for undoped NiO, 2Cu-NiO and 4Cu-NiO, respectively. Under UV radiation for 180 min., 4Cu-NiO nanocatalysts showed degradation efficiency of 66.36 and 47.00 % for 0.3 and 0.4 mol/L, respectively. After 300 min. of UV radiation, the maximum degradation efficiency was 66.83 % in 0.3 mol/L (4Cu-NiO), 75.20 and 72.04 % observed in 0.4 and 0.5 mol/L (2Cu-NiO). The maximum amount of phenol (75.2 %) was removed at 300 min.

References

[1] M. Nosuhi, A. Nezamzadeh-Ejhieh, High catalytic activity of Fe(II)-clinoptilolite nanoparticales for indirect voltammetric determination of dichromate: Experimental design by response surface methodology (RSM), Electrochimica Acta, 223 (2017) 47-62.

[2] A. Sharifi, L. Montazerghaem, A. Naeimi, A.R. Abhari, M. Vafaee, G.A.M. Ali, H. Sadegh, Investigation of photocatalytic behavior of modified ZnS:Mn/MWCNTs nanocomposite for

organic pollutants effective photodegradation, Journal of Environmental Management, 247 (2019) 624-632.

[3] A. Naghash, A. Nezamzadeh-Ejhieh, Comparison of the efficiency of modified clinoptilolite with HDTMA and HDP surfactants for the removal of phosphate in aqueous solutions, Journal of Industrial and Engineering Chemistry, 31 (2015) 185-191.

[4] S. Ahmed, M.G. Rasul, W.N. Martens, R. Brown, M.A. Hashib, Heterogeneous photocatalytic degradation of phenols in wastewater: A review on current status and developments, Desalination, 261 (2010) 3-18.

[5] M. Trillas, J. Peral, X. Domènech, Photo-oxidation of phenoxyacetic acid by TiO_2-illuminated catalyst, Applied Catalysis B: Environmental, 3 (1993) 45-53.

[6] F. Soori, A. Nezamzadeh-Ejhieh, Synergistic effects of copper oxide-zeolite nanoparticles composite on photocatalytic degradation of 2,6-dimethylphenol aqueous solution, Journal of Molecular Liquids, 255 (2018) 250-256.

[7] A. Nezamzadeh-Ejhieh, M. Bahrami, Investigation of the photocatalytic activity of supported ZnO–TiO_2 on clinoptilolite nano-particles towards photodegradation of wastewater-contained phenol, Desalination and Water Treatment, 55 (2015) 1096-1104.

[8] M. Giahi, D. Pathania, S. Agarwal, G.A.M. Ali, K.F. Chong, V.K. Gupta, Preparation of Mg-doped TiO_2 nanoparticles for photocatalytic degradation of some organic pollutants, Studia Universitatis Babes-Bolyai Chemia, 64 (2019) 7-18.

[9] I.H. Chowdhury, M. Roy, S. Kundu, M. Naskar, TiO_2 hollow microspheres impregnated with biogenic gold nanoparticles for the efficient visible light-induced photodegradation of phenol, Journal of Physics and Chemistry of Solids, 129 (2019) 329-339.

[10] T. Scott, H. Zhao, W. Deng, X. Feng, Y. Li, Photocatalytic degradation of phenol in water under simulated sunlight by an ultrathin MgO coated Ag/TiO_2 nanocomposite, Chemosphere, 216 (2019) 1-8.

[11] A. Nezamzadeh-Ejhieh, S. Khorsandi, Photocatalytic degradation of 4-nitrophenol with ZnO supported nano-clinoptilolite zeolite, Journal of Industrial and Engineering Chemistry, 20 (2014) 937-946.

[12] I. Oller, S. Malato, J.A. Sánchez-Pérez, Combination of advanced oxidation processes and biological treatments for wastewater decontamination-A review, Science of The Total Environment, 409 (2011) 4141-4166.

[13] A. Zhihui, Y. Peng, L. Xiaohua, Degradation of 4-Chlorophenol by microwave irradiation enhanced advanced oxidation processes, Chemosphere, 60 (2005) 824-827.

[14] T. Lai, C. Lee, K. Wu, Y. Shu, C. Wang, Microwave-enhanced catalytic degradation of phenol over nickel oxide, Applied Catalysis B: Environmental, 68 (2006) 147-153.

[15] N.F. Jaafar, Z.H. Ahmad, N.W.C. Jusoh, Y. Nagao, X-ray diffraction and spectroscopic studies of microwave synthesized mesoporous titania nanoparticles for photodegradation of 2-chlorophenol under visible light, AIP Conference Proceedings, AIP Publishing, 2019, pp. 020081.

[16] P. Wang, X. Bian, Y. Li, Catalytic oxidation of phenol in wastewater - A new application of the amorphous $Fe_{78}Si_9B_{13}$ alloy, Chinese Science Bulletin, 57 (2012) 33-40.

[17] N. Mahamuni, A. Pandit, Effect of additives on ultrasonic degradation of phenol, Ultrasonics Sonochemistry, 13 (2006) 165-174.

[18] M.H. Entezari, C. Pétrier, P. Devidal, Sonochemical degradation of phenol in water: a comparison of classical equipment with a new cylindrical reactor, Ultrasonics Sonochemistry, 10 (2003) 103-108.

[19] J. Lukáč, M. Klementová, P. Bezdička, S. Bakardjieva, J. Šubrt, L. Szatmáry, Z. Bastl, J. Jirkovský, Influence of Zr as TiO_2 doping ion on photocatalytic degradation of 4-chlorophenol, Applied Catalysis B: Environmental, 74 (2007) 83-91.

[20] H. Derikvandi, A. Nezamzadeh-Ejhieh, A comprehensive study on electrochemical and photocatalytic activity of SnO_2-ZnO/clinoptilolite nanoparticles, Journal of Molecular Catalysis A: Chemical, 426 (2017) 158-169.

[21] A. Pourtaheri, A. Nezamzadeh-Ejhieh, Photocatalytic properties of incorporated NiO onto clinoptilolite nano-particles in the photodegradation process of aqueous solution of cefixime pharmaceutical capsule, Chemical Engineering Research and Design, 104 (2015) 835-843.

[22] N.M.I. Alhaji, D. Nathiya, K. Kaviyarasu, M. Meshram, A. Ayeshamariam, A comparative study of structural and photocatalytic mechanism of $AgGaO_2$ nanocomposites for equilibrium and kinetics evaluation of adsorption parameters, Surfaces and Interfaces, 17 (2019) 100375.

[23] M. Pérez-Moya, M. Graells, L.J. del Valle, E. Centelles, H.D. Mansilla, Fenton and photo-Fenton degradation of 2-chlorophenol: Multivariate analysis and toxicity monitoring, Catalysis Today, 124 (2007) 163-171.

[24] X. Zhao, T. Xu, W. Yao, C. Zhang, Y. Zhu, Photoelectrocatalytic degradation of 4-chlorophenol at Bi_2WO_6 nanoflake film electrode under visible light irradiation, Applied Catalysis B: Environmental, 72 (2007) 92-97.

[25] A. Nezamzadeh-Ejhieh, M. Khorsandi, Heterogeneous photodecolorization of Eriochrome Black T using Ni/P zeolite catalyst, Desalination, 262 (2010) 79-85.

[26] V.K. Gupta, S. Agarwal, H. Sadegh, G.A.M. Ali, A.K. Bharti, A.S. Hamdy Makhlouf, Facile route synthesis of novel graphene oxide-β-cyclodextrin nanocomposite and its application as adsorbent for removal of toxic bisphenol A from the aqueous phase, Journal of Molecular Liquids, 237 (2017) 466-472.

[27] M.M. Ba-Abbad, A.A.H. Kadhum, A.B. Mohamad, M.S. Takriff, K. Sopian, Synthesis and catalytic activity of TiO_2 nanoparticles for photochemical oxidation of concentrated chlorophenols under direct solar radiation, International Journal of Electrochemical Science, 7 (2012) 4871-4888.

[28] M. Wang, J. Han, Y. Hu, R. Guo, Y. Yin, Carbon-incorporated NiO/TiO_2 mesoporous shells with p–n heterojunctions for efficient visible light photocatalysis, ACS Applied Materials & Interfaces, 8 (2016) 29511-29521.

[29] S. Esplugas, J. Giménez, S. Contreras, E. Pascual, M. Rodríguez, Comparison of different advanced oxidation processes for phenol degradation, Water Research, 36 (2002) 1034-1042.

[30] A.M. Abdullah, N.J. Al-Thani, K. Tawbi, H. Al-Kandari, Carbon/nitrogen-doped TiO_2: New synthesis route, characterization and application for phenol degradation, Arabian Journal of Chemistry, 9 (2016) 229-237.

[31] A. Sharma, B.-K. Lee, Integrated ternary nanocomposite of TiO_2/NiO/reduced graphene oxide as a visible light photocatalyst for efficient degradation of o-chlorophenol, Journal of Environmental Management, 181 (2016) 563-573.

[32] P. Xiong, Y. Fu, L. Wang, X. Wang, Multi-walled carbon nanotubes supported nickel ferrite: A magnetically recyclable photocatalyst with high photocatalytic activity on degradation of phenols, Chemical Engineering Journal, 195-196 (2012) 149-157.

[33] H. Labiadh, T.B. Chaabane, L. Balan, N. Becheik, S. Corbel, G. Medjahdi, R. Schneider, Preparation of Cu-doped ZnS QDs/TiO_2 nanocomposites with high photocatalytic activity, Applied Catalysis B: Environmental, 144 (2014) 29-35.

[34] N. Arabpour, A. Nezamzadeh-Ejhieh, Photodegradation of cotrimaxazole by clinoptilolite-supported nickel oxide, Process Safety and Environmental Protection, 102 (2016) 431-440.

[35] K. Hayat, M.A. Gondal, M.M. Khaled, S. Ahmed, Effect of operational key parameters on photocatalytic degradation of phenol using nano nickel oxide synthesized by sol–gel method, Journal of Molecular Catalysis A: Chemical, 336 (2011) 64-71.

[36] M. Aliahmad, A. Rahdar, Y. Azizi, Synthesis of Cu doped NiO nanoparticles by chemical method, Journal of Nanostructures, 4 (2014) 145-152.

[37] S. Senobari, A. Nezamzadeh-Ejhieh, A p-n junction NiO-CdS nanoparticles with enhanced photocatalytic activity: A response surface methodology study, Journal of Molecular Liquids, 257 (2018) 173-183.

[38] A. Patterson, The Scherrer formula for X-ray particle size determination, Physical Review, 56 (1939) 978-982.

[39] M. Kanthimathi, A. Dhathathreyan, B.U. Nair, Nanosized nickel oxide using bovine serum albumin as template, Materials Letters, 58 (2004) 2914-2917.

[40] K. Kaviyarasu, E. Manikandan, J. Kennedy, M. Jayachandran, R. Ladchumananandasiivam, U.U. De Gomes, M. Maaza, Synthesis and characterization studies of NiO nanorods for enhancing solar cell efficiency using photon upconversion materials, Ceramics International, 42 (2016) 8385-8394.

[41] D. Petrov, S. Christoskova, M. Stoyanova, V. Ivanova, D. Karashanova, Preparation, characterization and catalytic activity of NiO_x and NiO_x/ZrO_2 for oxidation of phenol in aqueous solution, Acta Chimica Slovenica, 61 (2014) 759-770.

[42] O.A. Fouad, S.A. Makhlouf, G.A.M. Ali, A.Y. El-Sayed, Cobalt/silica nanocomposite via thermal calcination-reduction of gel precursors, Materials Chemistry and Physics, 128 (2011) 70-76.

[43] G.A.M. Ali, O.A. Fouad, S.A. Makhlouf, Structural, optical and electrical properties of sol-gel prepared mesoporous Co_3O_4/SiO_2 nanocomposites, Journal of Alloys and Compounds, 579 (2013) 606-611.

[44] M. Babaahamdi-Milani, A. Nezamzadeh-Ejhieh, A comprehensive study on photocatalytic activity of supported Ni/Pb sulfide and oxide systems onto natural zeolite nanoparticles, Journal of Hazardous Materials, 318 (2016) 291-301.

[45] H. Derikvandi, A. Nezamzadeh-Ejhieh, Designing of experiments for evaluating the interactions of influencing factors on the photocatalytic activity of NiS and SnS_2: Focus on coupling, supporting and nanoparticles, Journal of Colloid and Interface Science, 490 (2017) 628-641.

[46] K. Kaviyarasu, L. Kotsedi, A. Simo, X. Fuku, G.T. Mola, J. Kennedy, M. Maaza, Photocatalytic activity of ZrO_2 doped lead dioxide nanocomposites: Investigation of structural and optical microscopy of RhB organic dye, Applied Surface Science, 421 (2017) 234-239.

[47] C.M. Magdalane, K. Kaviyarasu, G.M.A. Priyadharsini, A.K.H. Bashir, N. Mayedwa, N. Matinise, A.B. Isaev, N. Abdullah Al-Dhabi, M.V. Arasu, S. Arokiyaraj, J. Kennedy, M. Maaza, Improved photocatalytic decomposition of aqueous Rhodamine-B by solar light illuminated

hierarchical yttria nanosphere decorated ceria nanorods, Journal of Materials Research and Technology, 8 (2019) 2898-2909.

[48] N. Bayal, P. Jeevanandam, Synthesis of CuO@NiO core-shell nanoparticles by homogeneous precipitation method, Journal of Alloys and Compounds, 537 (2012) 232-241.

[49] O.A. Fouad, G.A.M. Ali, M.A.I. El-Erian, S.A. Makhlouf, Humidity sensing properties of cobalt oxide/silica nanocomposites prepared via sol-gel and related routes, Nano, 7 (2012) 1250038.

[50] A. Nezamzadeh-Ejhieh, E. Afshari, Modification of a PVC-membrane electrode by surfactant modified clinoptilolite zeolite towards potentiometric determination of sulfide, Microporous and Mesoporous Materials, 153 (2012) 267-274.

[51] K.K. Purushothaman, G. Muralidharan, The effect of annealing temperature on the electrochromic properties of nanostructured NiO films, Solar Energy Materials and Solar Cells, 93 (2009) 1195-1201.

[52] A. Patra, K. Auddy, D. Ganguli, J. Livage, P.K. Biswas, Sol–gel electrochromic WO_3 coatings on glass, Materials Letters, 58 (2004) 1059-1063.

[53] F. Davar, Z. Fereshteh, M. Salavati-Niasari, Nanoparticles Ni and NiO: Synthesis, characterization and magnetic properties, Journal of Alloys and Compounds, 476 (2009) 797-801.

[54] A. Angel Ezhilarasi, J. Judith Vijaya, K. Kaviyarasu, L. John Kennedy, R.J. Ramalingam, H.A. Al-Lohedan, Green synthesis of NiO nanoparticles using Aegle marmelos leaf extract for the evaluation of in-vitro cytotoxicity, antibacterial and photocatalytic properties, Journal of Photochemistry and Photobiology B: Biology, 180 (2018) 39-50.

[55] S. Al-Amri, M. Ansari, S. Rafique, M. Aldhahri, S. Rahimuddin, A. Azam, A. Memic, Ni doped CuO nanoparticles: structural and optical characterizations, Current Nanoscience, 11 (2015) 191-197.

[56] M. Faisal, S.B. Khan, M.M. Rahman, A. Jamal, A. Umar, Ethanol chemi-sensor: Evaluation of structural, optical and sensing properties of CuO nanosheets, Materials Letters, 65 (2011) 1400-1403.

[57] C. Maria Magdalane, K. Kaviyarasu, J. Judith Vijaya, B. Siddhardha, B. Jeyaraj, Facile synthesis of heterostructured cerium oxide/yttrium oxide nanocomposite in UV light induced photocatalytic degradation and catalytic reduction: Synergistic effect of antimicrobial studies, Journal of Photochemistry and Photobiology B: Biology, 173 (2017) 23-34.

[58] K. Anand, K. Kaviyarasu, S. Muniyasamy, S.M. Roopan, R.M. Gengan, A.A. Chuturgoon, Bio-Synthesis of Silver Nanoparticles Using Agroforestry Residue and Their Catalytic Degradation for Sustainable Waste Management, Journal of Cluster Science, 28 (2017) 2279-2291.

[59] M.A. Gondal, M.N. Sayeed, A. Alarfaj, Activity comparison of Fe_2O_3, NiO, WO_3, TiO_2 semiconductor catalysts in phenol degradation by laser enhanced photo-catalytic process, Chemical Physics Letters, 445 (2007) 325-330.

[60] S. Rengaraj, X.Z. Li, Enhanced photocatalytic activity of TiO_2 by doping with Ag for degradation of 2,4,6-trichlorophenol in aqueous suspension, Journal of Molecular Catalysis A: Chemical, 243 (2006) 60-67.

[61] D. de la Cruz Romero, G.T. Torres, J.C. Arévalo, R. Gomez, A. Aguilar-Elguezabal, Synthesis and characterization of TiO_2 doping with rare earths by sol–gel method: photocatalytic activity for phenol degradation, Journal of Sol-Gel Science and Technology, 56 (2010) 219-226.

[62] M.A. Barakat, H. Schaeffer, G. Hayes, S. Ismat-Shah, Photocatalytic degradation of 2-chlorophenol by Co-doped TiO_2 nanoparticles, Applied Catalysis B: Environmental, 57 (2005) 23-30.

[63] A.-W. Xu, Y. Gao, H.-Q. Liu, The preparation, characterization, and their photocatalytic activities of rare-earth-doped TiO_2 nanoparticles, Journal of Catalysis, 207 (2002) 151-157.

[64] A. Burns, W. Li, C. Baker, S.I. Shah, Sol-gel synthesis and characterization of neodymium-ion doped nanostructured titania thin films, MRS Proceedings, 703 (2001).

[65] X.-J. Yang, S. Wang, H.-M. Sun, X.-B. Wang, J.-S. Lian, Preparation and photocatalytic performance of Cu-doped TiO_2 nanoparticles, Transactions of Nonferrous Metals Society of China, 25 (2015) 504-509.

[66] C.-H. Chiou, R.-S. Juang, Photocatalytic degradation of phenol in aqueous solutions by Pr-doped TiO_2 nanoparticles, Journal of Hazardous Materials, 149 (2007) 1-7.

[67] Y.B. Feng, L. Hong, A.L. Liu, W.D. Chen, G.W. Li, W. Chen, X.H. Xia, High-efficiency catalytic degradation of phenol based on the peroxidase-like activity of cupric oxide nanoparticles, International Journal of Environmental Science and Technology, 12 (2013) 653-660.

[68] R.-a. Doong, W.-h. Chang, Photodegradation of parathion in aqueous titanium dioxide and zero valent iron solutions in the presence of hydrogen peroxide, Journal of Photochemistry and Photobiology A: Chemistry, 116 (1998) 221-228.

[69] J. Ye, X. Li, J. Hong, J. Chen, Q. Fan, Photocatalytic degradation of phenol over ZnO nanosheets immobilized on montmorillonite, Materials Science in Semiconductor Processing, 39 (2015) 17-22.

[70] A. Nezamzadeh-Ejhieh, S. Hushmandrad, Solar photodecolorization of methylene blue by CuO/X zeolite as a heterogeneous catalyst, Applied Catalysis A: General, 388 (2010) 149-159.

[71] Y. Subba Reddy, C. Maria Magdalane, K. Kaviyarasu, G.T. Mola, J. Kennedy, M. Maaza, Equilibrium and kinetic studies of the adsorption of acid blue 9 and Safranin O from aqueous solutions by MgO decked FLG coated Fuller's earth, Journal of Physics and Chemistry of Solids, 123 (2018) 43-51.

[72] M. Choquette-Labbé, W. Shewa, J. Lalman, S. Shanmugam, Photocatalytic degradation of phenol and phenol derivatives using a nano-TiO_2 catalyst: Integrating quantitative and qualitative factors using response surface methodology, Water, 6 (2014) 1785-1806.

[73] Z. Xiong, L.L. Zhang, X.S. Zhao, Visible-light-induced dye degradation over copper-modified reduced graphene oxide, Chemistry - A European Journal, 17 (2011) 2428-2434.

[74] H. Derikvandi, A. Nezamzadeh-Ejhieh, Increased photocatalytic activity of NiO and ZnO in photodegradation of a model drug aqueous solution: Effect of coupling, supporting, particles size and calcination temperature, Journal of Hazardous Materials, 321 (2017) 629-638.

[75] S. Senobari, A. Nezamzadeh-Ejhieh, A comprehensive study on the enhanced photocatalytic activity of CuO-NiO nanoparticles: Designing the experiments, Journal of Molecular Liquids, 261 (2018) 208-217.

[76] H. Derikvandi, A. Nezamzadeh-Ejhieh, Synergistic effect of p-n heterojunction, supporting and zeolite nanoparticles in enhanced photocatalytic activity of NiO and SnO2, Journal of Colloid and Interface Science, 490 (2017) 314-327.

[77] S.-M. Lam, J.-C. Sin, A.Z. Abdullah, A.R. Mohamed, Degradation of wastewaters containing organic dyes photocatalysed by zinc oxide: a review, Desalination and Water Treatment, 41 (2012) 131-169.

[78] J.-C. Sin, S.-M. Lam, A.R. Mohamed, K.-T. Lee, Degrading endocrine disrupting chemicals from wastewater by photocatalysis: A Review, International Journal of Photoenergy, 2012 (2012) 1-23.

[79] Z. Fan, F. Meng, J. Gong, H. Li, Z. Ding, B. Ding, One-step hydrothermal synthesis of mesoporous Ce-doped anatase TiO_2 nanoparticles with enhanced photocatalytic activity, Journal of Materials Science: Materials in Electronics, 27 (2016) 11866-11872.

[80] V. Krishnakumar, S. Boobas, J. Jayaprakash, M. Rajaboopathi, B. Han, M. Louhi-Kultanen, Effect of Cu doping on TiO_2 nanoparticles and its photocatalytic activity under visible light, Journal of Materials Science: Materials in Electronics, 27 (2016) 7438-7447.

List of Tables:

Table 1. Average crystallite size, interplanar distance, lattice parameters and bandgap of NiO and doped samples as listed below.

Sample name	Average crystallite size from XRD (nm)	Interplanar distance (nm)	Lattice parameters (nm)	Average particle size from TEM (nm)	Bandgap (eV)
NiO	24	0.2442	0.488	28.0	3.26
2Cu-NiO	22.8	0.2241	0.448	26.6	3.64
4Cu-NiO	19.03	0.2125	0.425	22.8	3.87

Table 2. Kinetic constant and regression coefficients of phenol degradation for 3 and 5 h with respect to different concentrations of phenol and nanocatalyst.

Samples	3 h		5 h	
	K_{app} (min.$^{-1}$)	R^2	K_{app} (min.$^{-1}$)	R^2
NiO (0.3 mol/L)	0.00136	0.9919	0.00198	0.9971
NiO (0.4 mol/L)	0.00203	0.9659	0.00175	0.9801
NiO (0.5 mol/L)	0.00346	0.9765	0.00342	0.9961
2Cu-NiO (0.3 mol/L)	0.00382	0.9888	0.00296	0.9887
2Cu-NiO (0.4 mol/L)	0.00266	0.9887	0.0047	0.9777
2Cu-NiO (0.5 mol/L)	0.00200	0.9889	0.00425	0.9875
4Cu-NiO (0.3 mol/L)	0.00603	0.9955	0.00365	0.9813
4Cu-NiO (0.4 mol/L)	0.00353	0.9825	0.00209	0.9648
4Cu-NiO (0.5 mol/L)	0.00144	0.9768	0.00276	0.9624

Table 3. Photocatalytic activity of undoped and doped NiO for photodegradation of phenol

Sample	**3 h**	**5 h**
NiO (0.3 mol/L)	22.05	44.96
NiO (0.4 mol/L)	30.56	46.82
NiO (0.5 mol/L)	26.31	34.05
2Cu-NiO (0.3 mol/L)	49.61	58.77
2Cu-NiO (0.4 mol/L)	37.55	47.56
2Cu-NiO (0.5 mol/L)	25.03	41.39
4Cu-NiO (0.3 mol/L)	66.38	75.23
4Cu-NiO (0.4 mol/L)	47.20	66.83
4Cu-NiO (0.5 mol/L)	23.15	56.70

List of Figures:

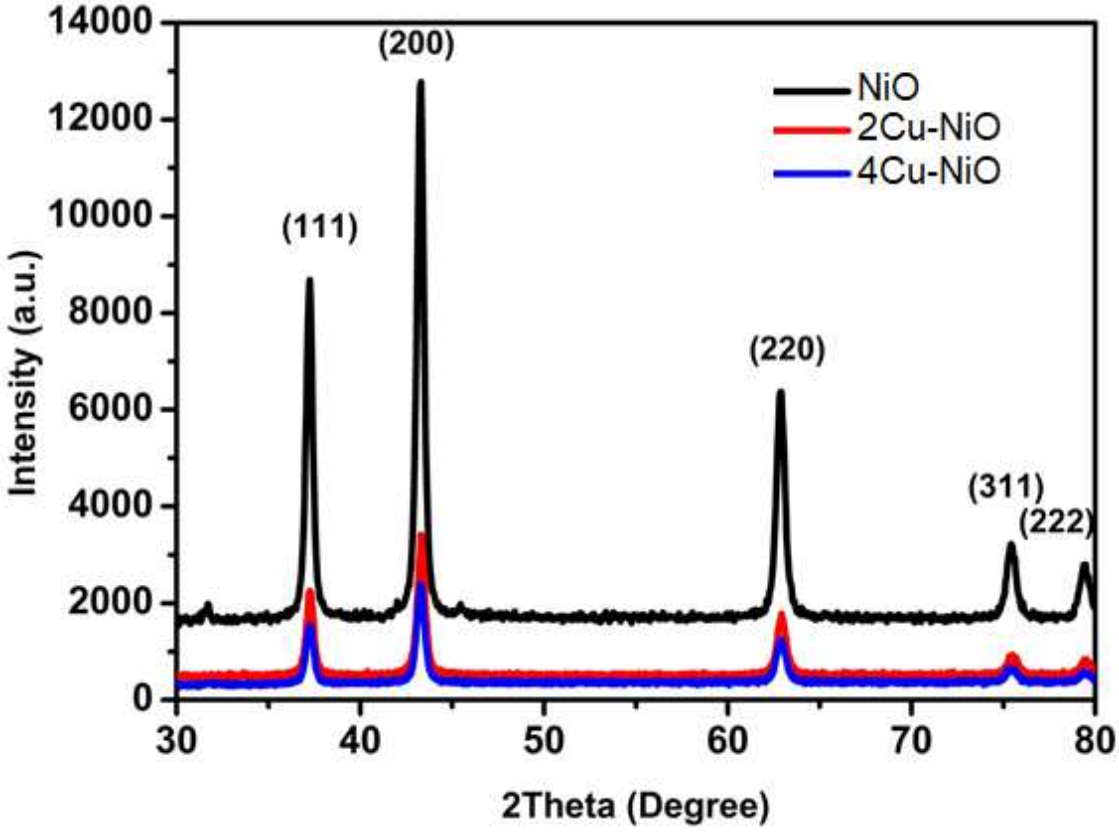

Fig. 1. XRD spectra of undoped NiO and Cu doped NiO NPs.

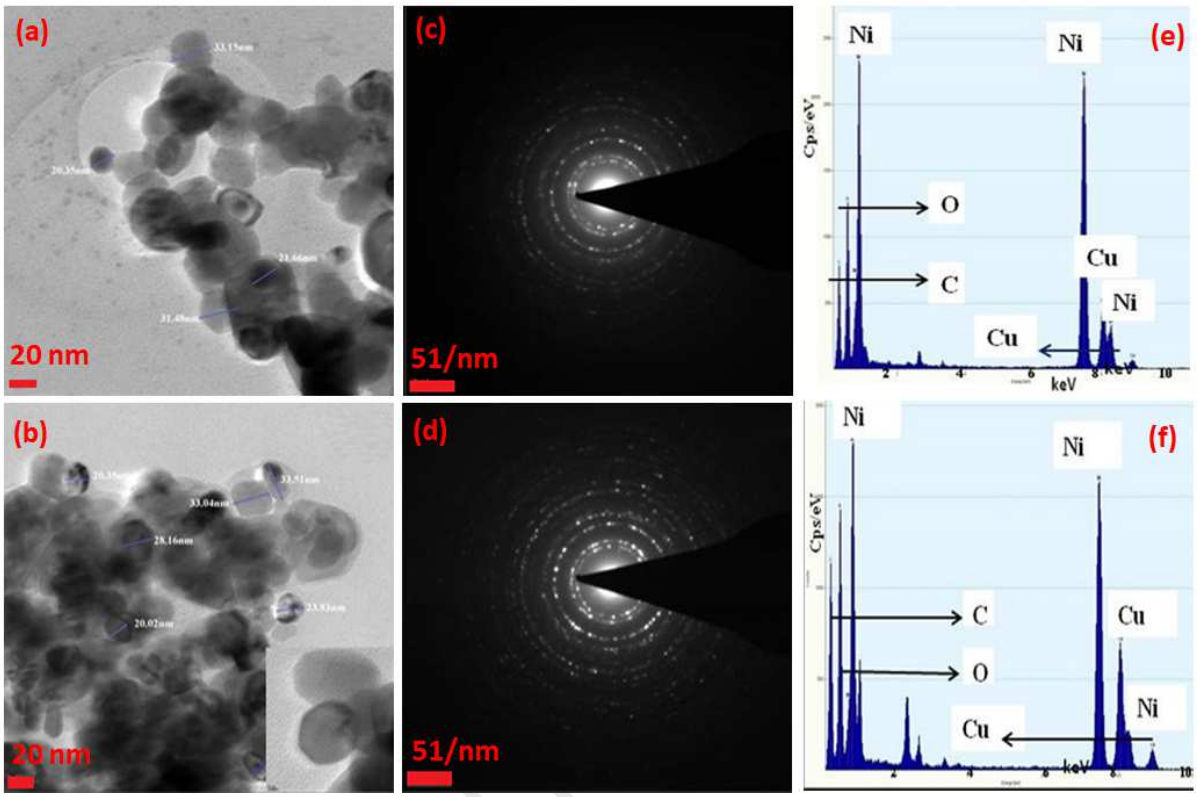

Fig. 2. TEM images (a and b), SAED patterns (c and d) and EDS spectra (e and f), respectively, for 2Cu-NiO and 4Cu-NiO.

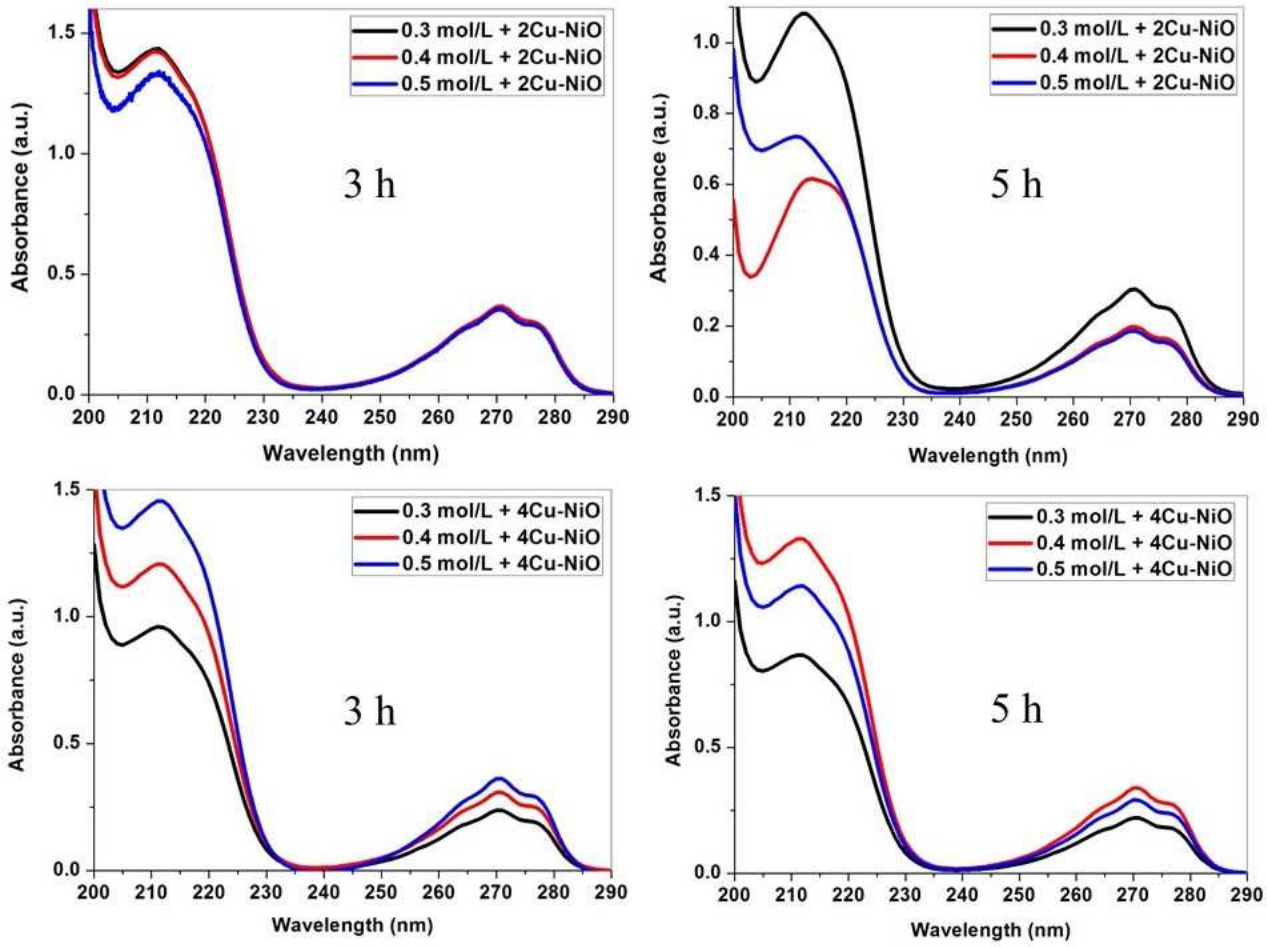

Fig. 3. UV-Vis spectra overlay graphs of phenol degradation in the presence of 2Cu-NiO and 4Cu-NiO in different phenol concentrations (0.3, 0.4, 0.5 mole/L) for 3 h and 5 h.

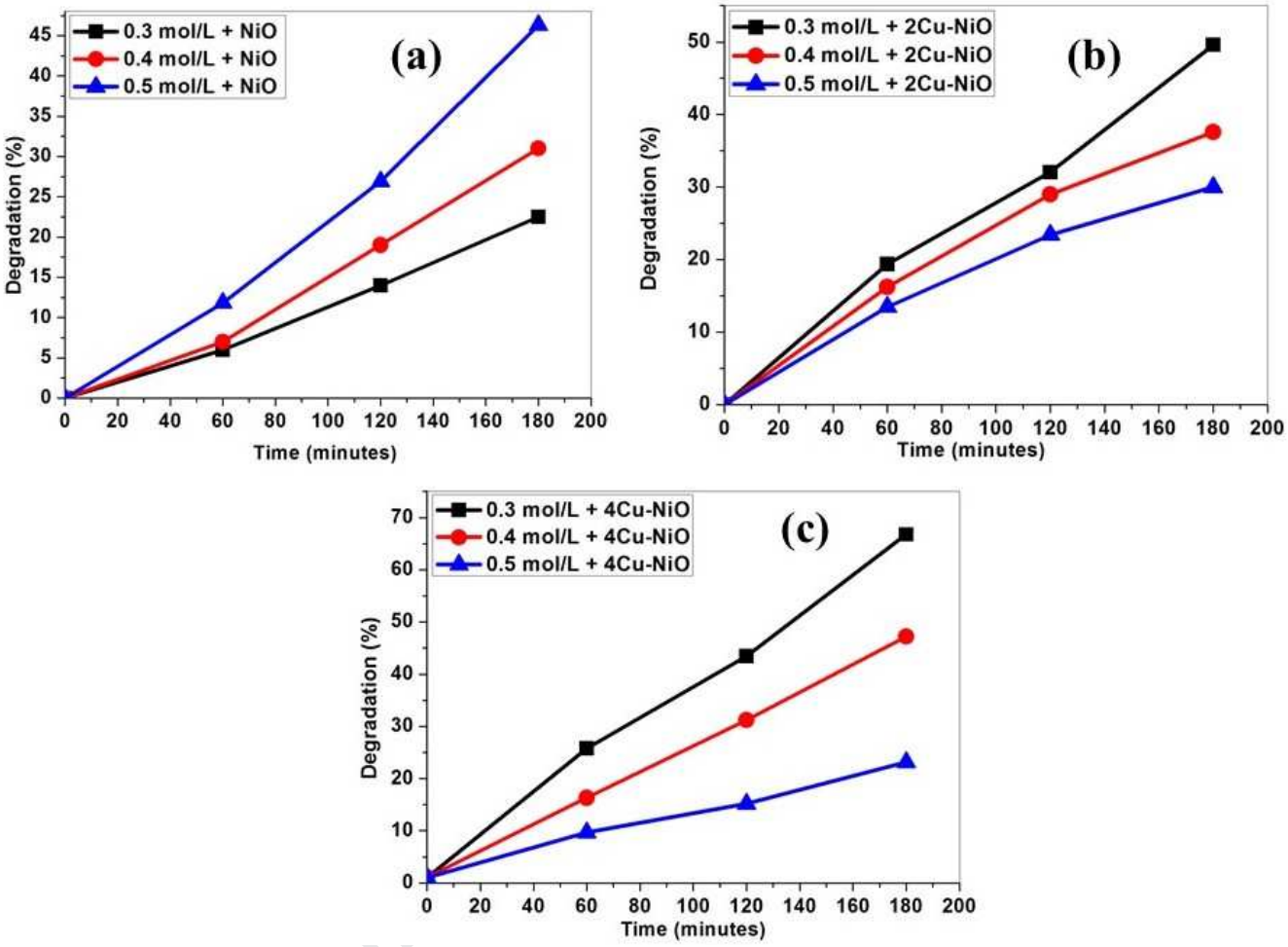

Fig. 4. Plot of photodegradation versus irradiation time for 0.3, 0.4 and 0.5 mol/L of phenol concentrations at 3 h (a) NiO, (b) 2Cu-NiO and (c) 4Cu-NiO.

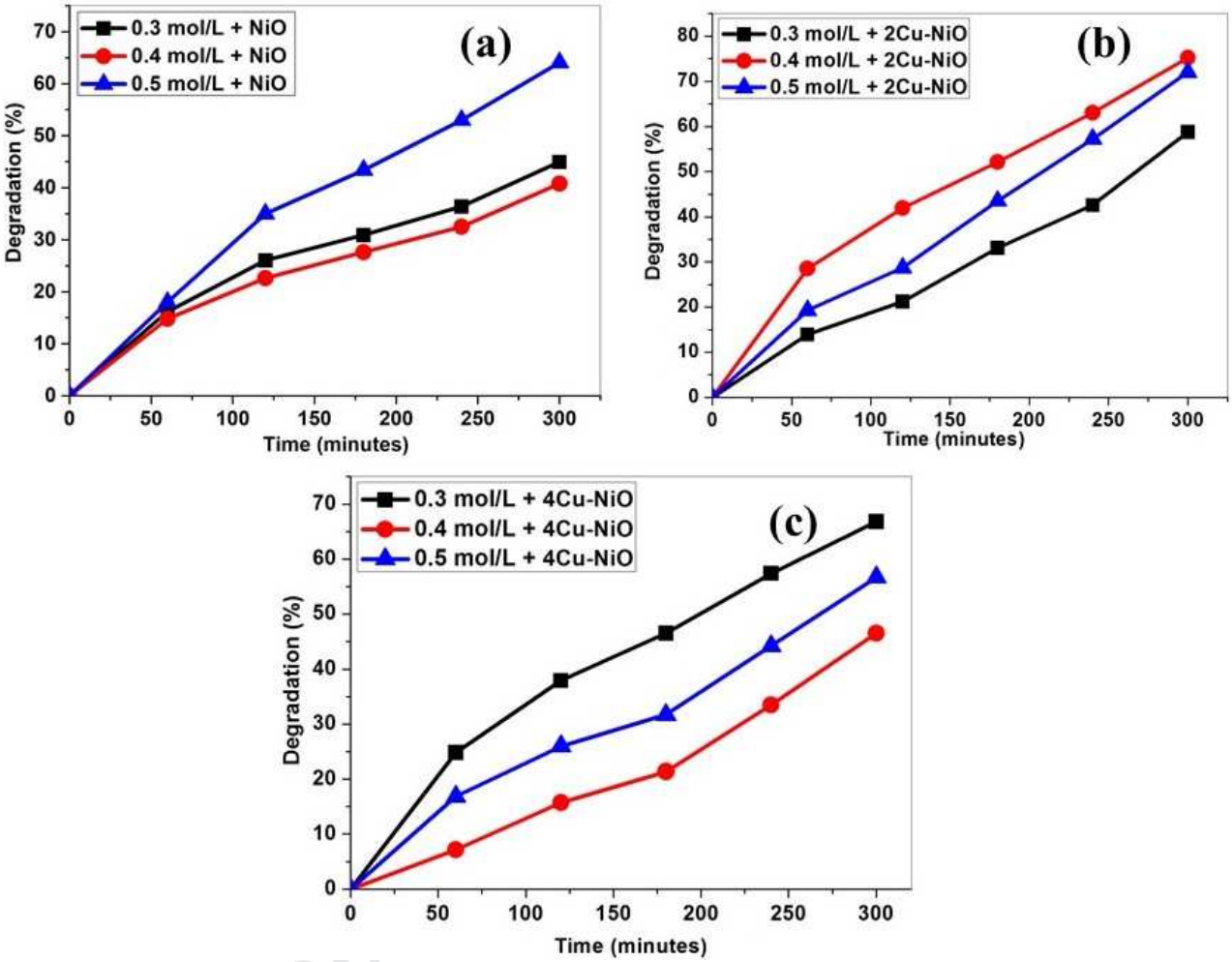

Fig. 5. Plot of photodegradation versus irradiation time for 0.3, 0.4 and 0.5 mol/L of phenol concentrations at 5 h (a) NiO, (b) 2Cu-NiO and (c) 4Cu-NiO.

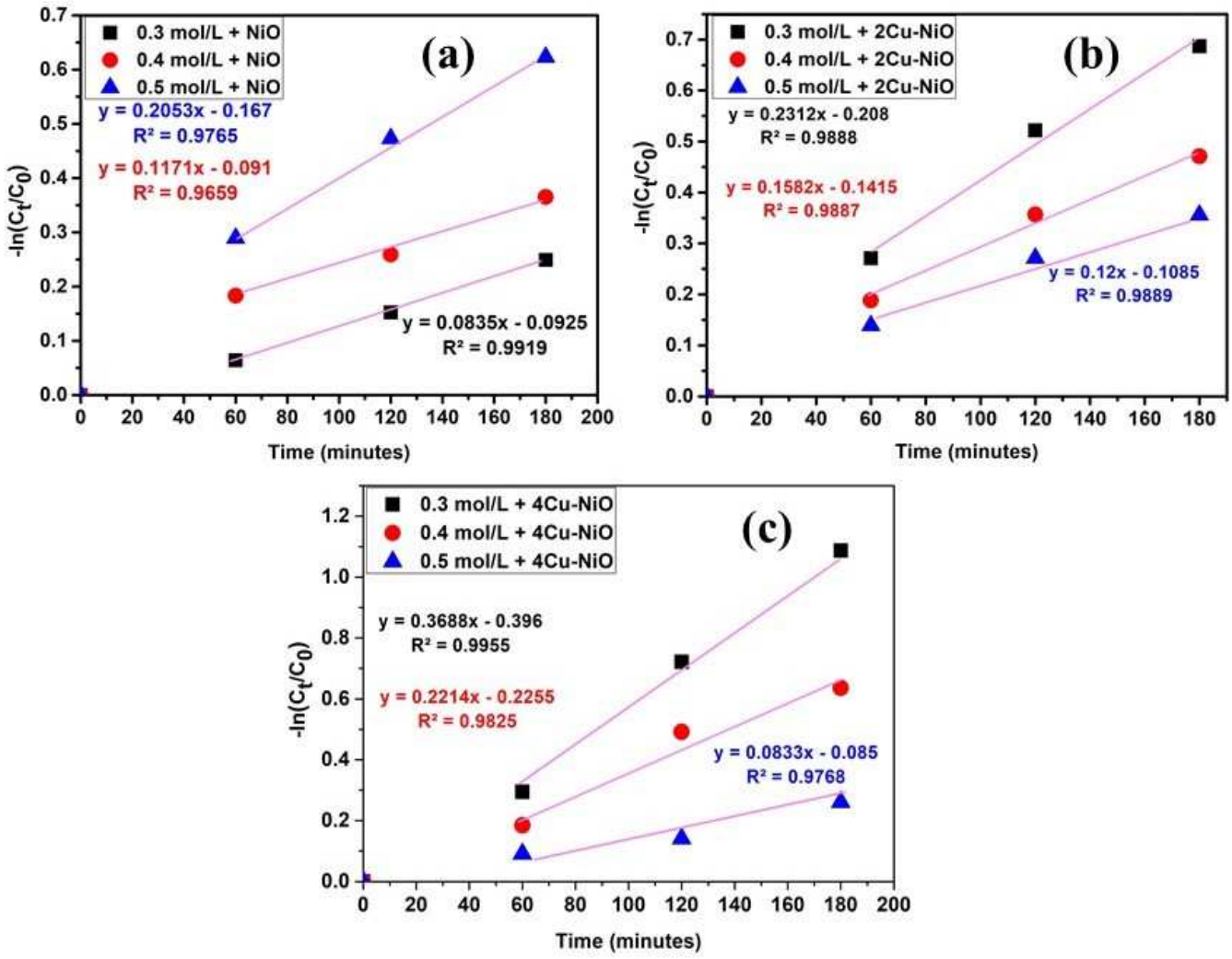

Fig. 6. Plot of $-\ln(C_t/C_o)$ versus time for the optimization of nanocatalysts for 3 h (a) NiO, (b) 2Cu-NiO, and (c) 4Cu-NiO.

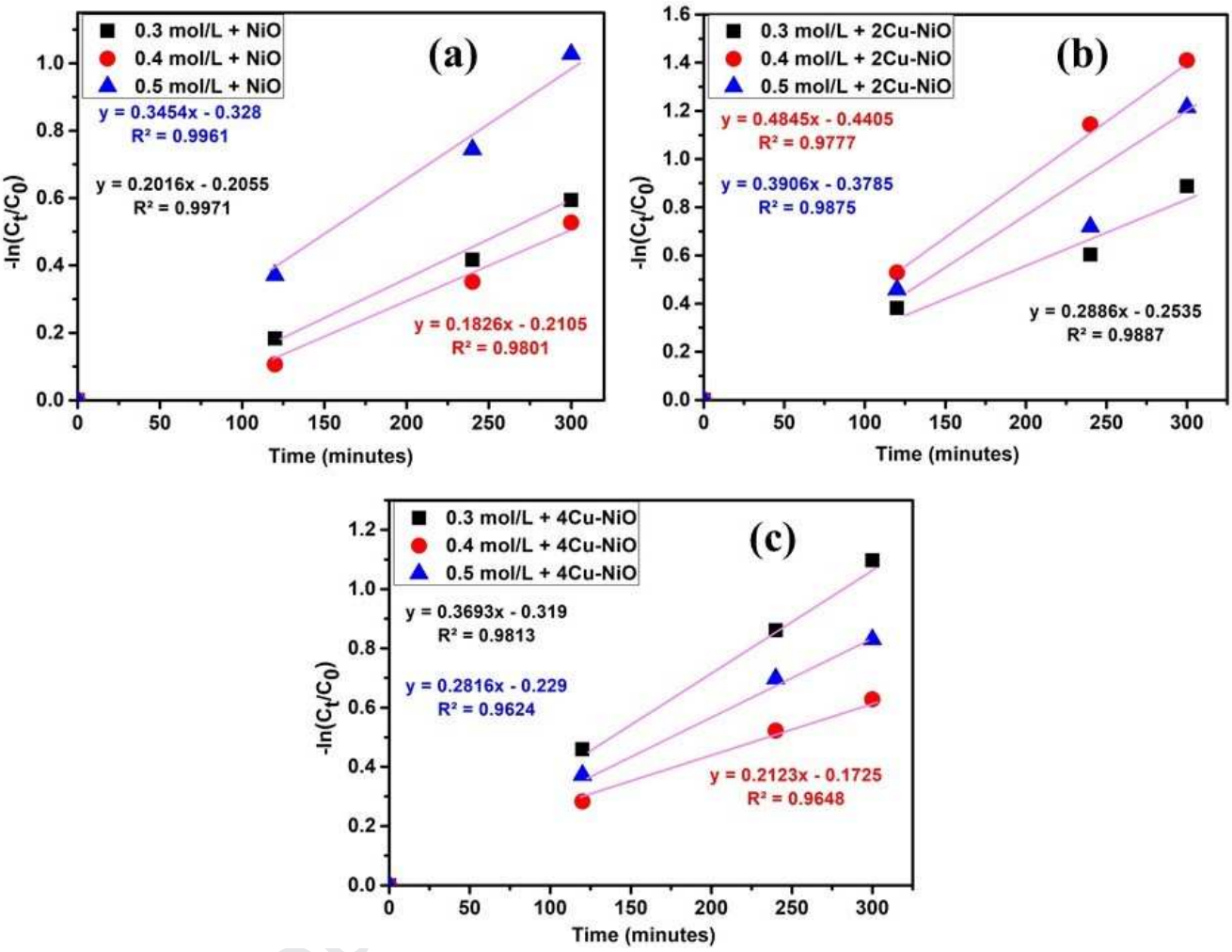

Fig. 7. Plot of $-\ln(C_t/C_o)$ versus time for the optimization of nanocatalysts for 5 h (a) NiO, (b) 2Cu-NiO and (c) 4Cu-NiO.

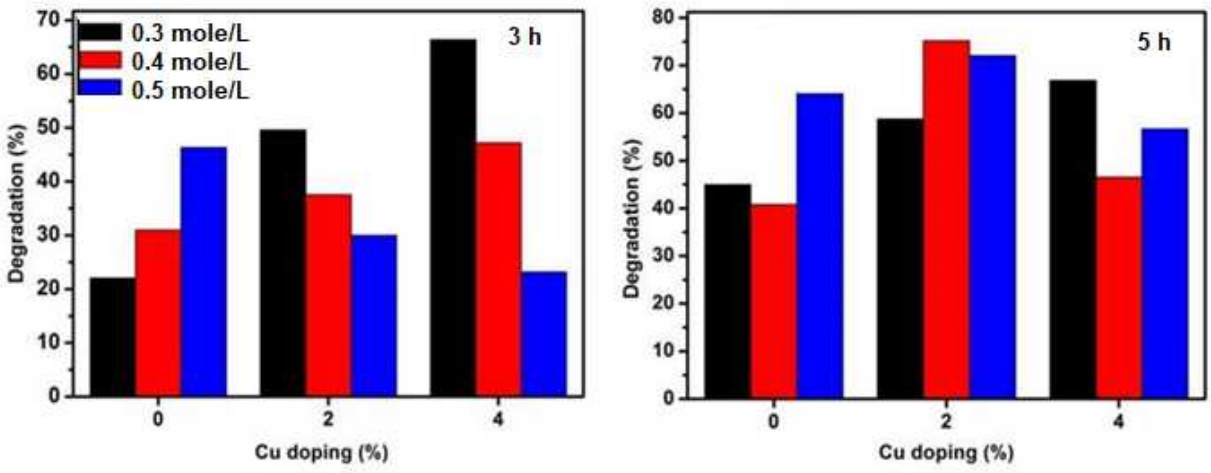

Fig. 8. Degradation of phenol versus doping ratio of Cu.

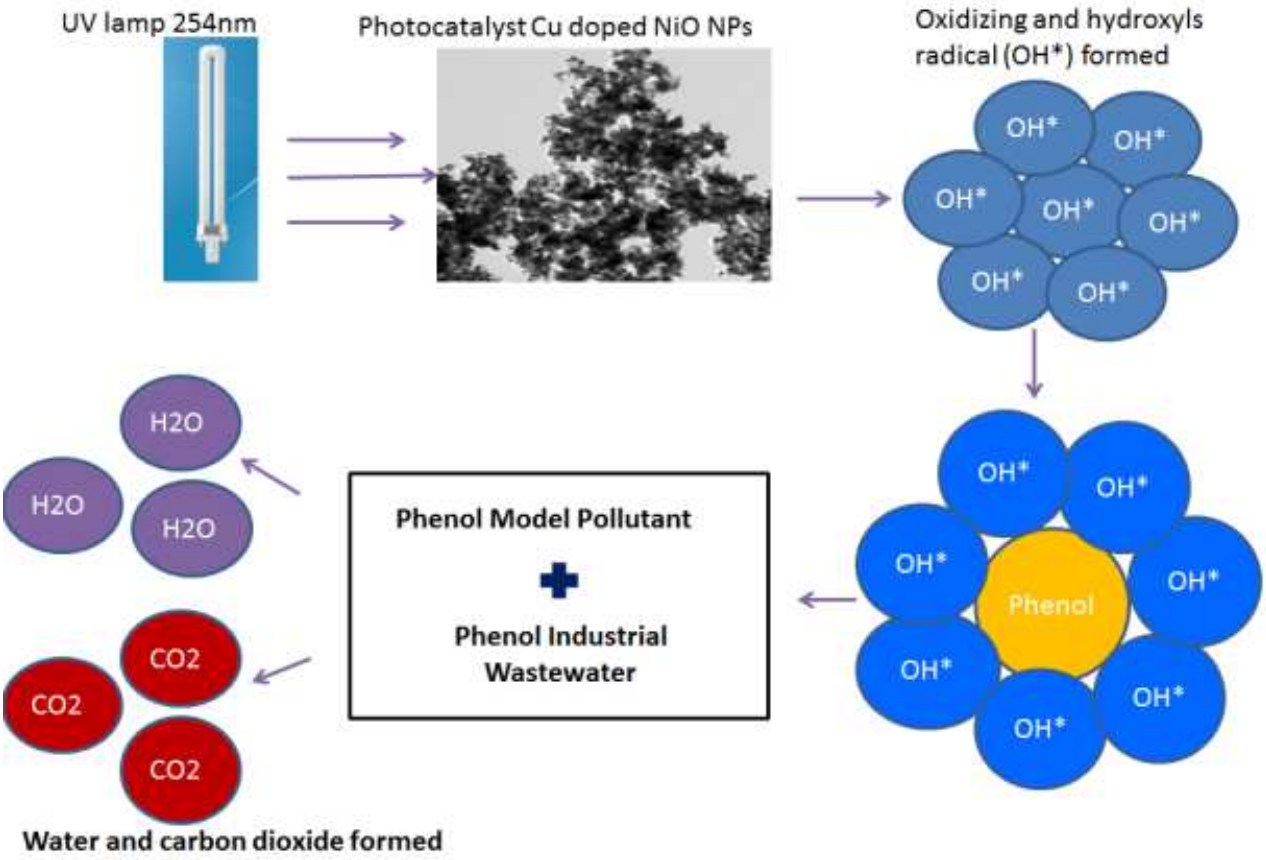

Fig. 9. Schematic diagram for phenol photodegradation mechanism by nanocatalysts.

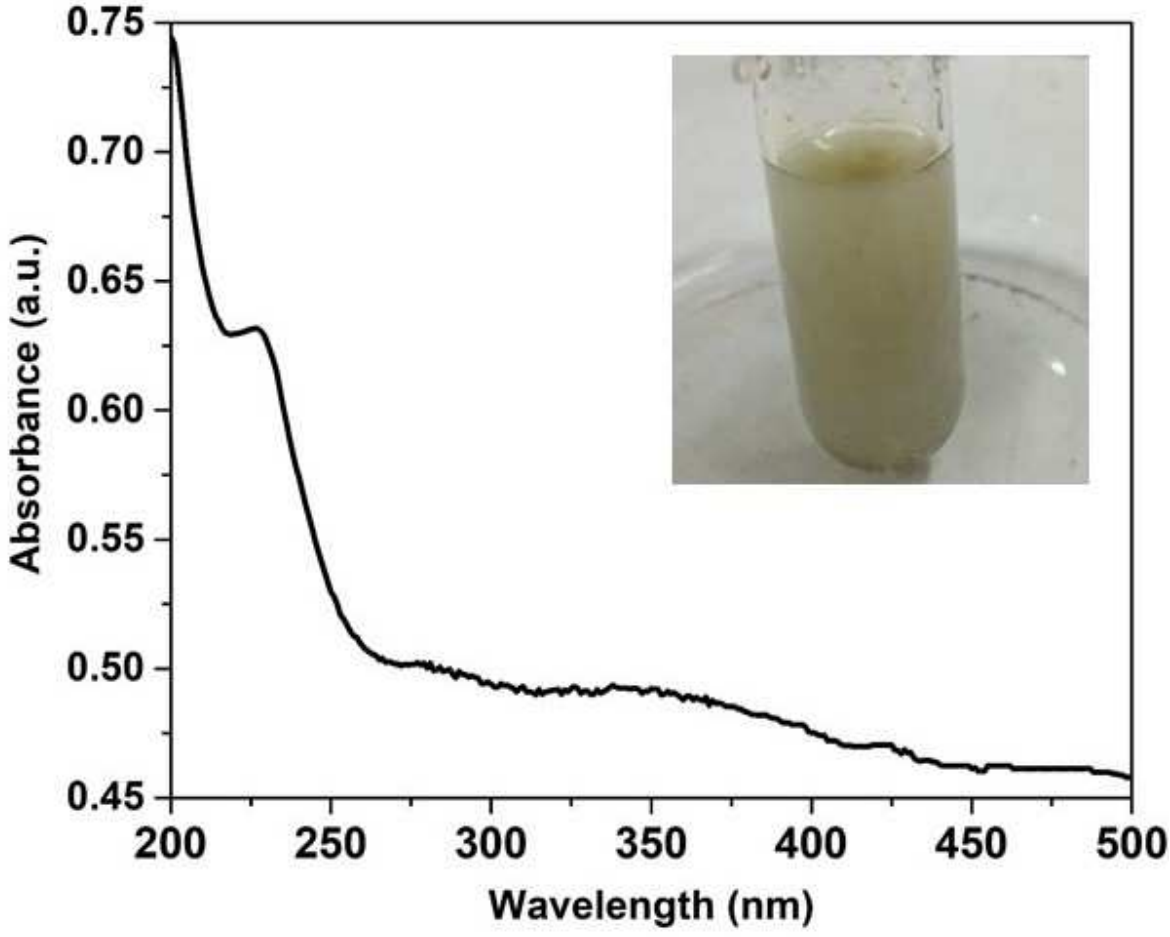

Fig. 10. Optical absorption spectrum of the industrial wastewater and the inset represents the photograph of the leather industries real effluent sample.

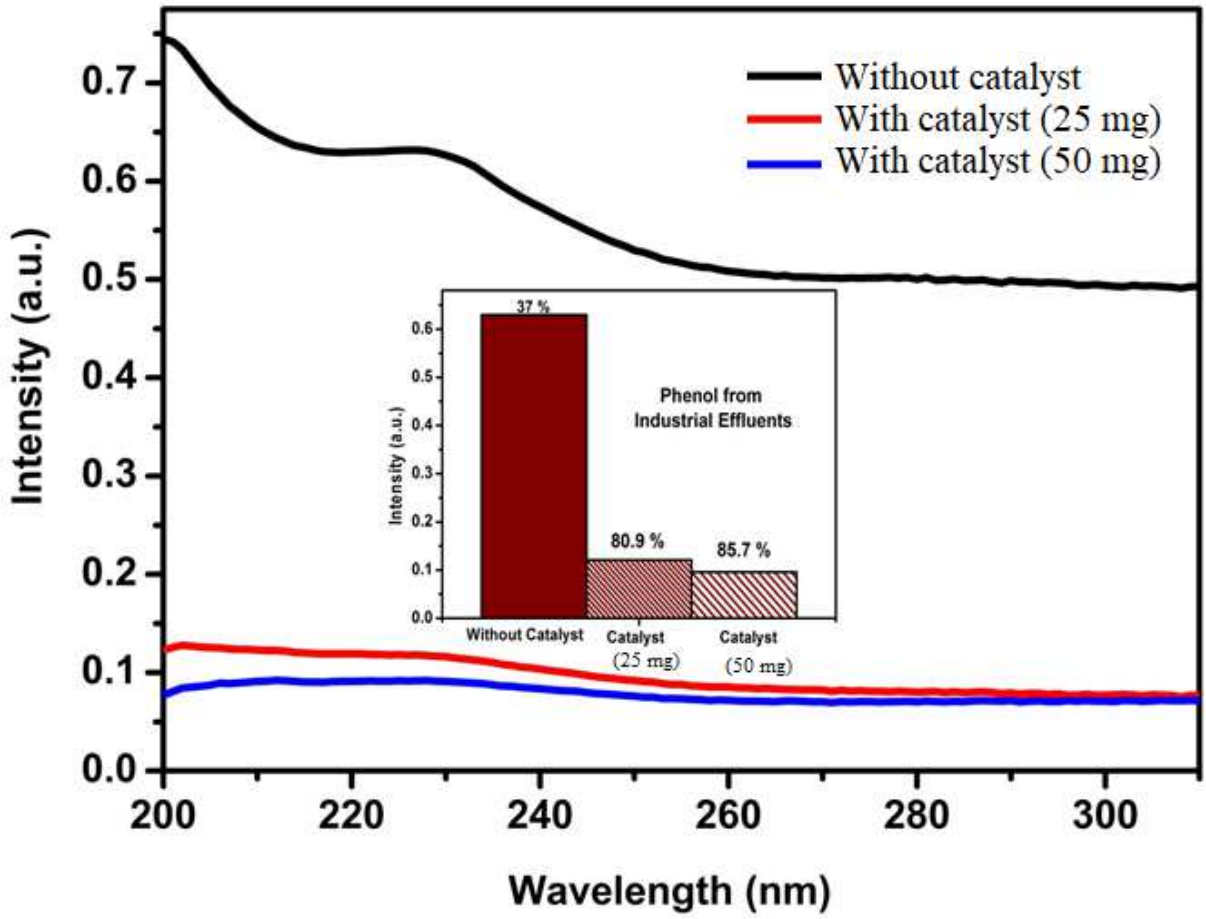

Fig. 11. Degradation spectra of the industrial wastewater (without catalyst, with the catalyst (25 mg) and with the catalyst (50 mg)).

Photocatalytic performance of a novel semiconductor nanocatalyst: Copper doped nickel oxide for phenol degradation

Anita Sagadevan Ethiraj [1, 2,]*, Prateek Uttam [2], Varunkumar K. [2], Kwok Feng Chong [3], Gomaa A. M. Ali [3,4,]

Highlights:

- Cu-NiO nanocatalysts showed a particles size in the range of 22 to 26 nm
- Nanocatalysts showed an energy bandgap in the range of 3.64-3.87 eV
- Cu-NiO nanocatalysts utilized for phenolic compounds degradation
- The maximum degradation efficiency was 75.2% observed in 0.4 mole/L

13th Nov 2019

Dear Editor,

We would like to express our pleasure in submitting the enclosed revised manuscript entitled “Photocatalytic performance of a novel semiconductor nanocatalyst: Copper doped nickel oxide for phenol degradation” for consideration for publication in *Mateials Chemisty and Physics.*

We confirm this work to be original, which neither has been published in the past, nor is currently under consideration for publication elsewhere. Furthermore, all the authors of this paper have approved the submission and have no conflict of interest to disclose.

We deeply appreciate your consideration of our revised manuscript and look forward to hearing from you in due course. Please address all correspondence concerning this manuscript to me at ethirajanita25@gmail.com.

Thanking you

Sincerely,

Anita S Ethiraj
Department of Physics
VIT-AP University, Amaravati
Andhra Pradesh 522237,
India